ACS OMEGA

http://pubs.acs.org/journal/acsodf

Article

# Surface Gelatin-Coated β-Mannanase-Immobilized Lignin for Delayed Release of β-Mannanase to Remediate Guar-Based Fracturing Fluid Damage

Haonan Cong, Zihao Ma, Meixi Hu, Junjie Han, Xing Wang,* Ying Han,* Yao Li, and Guangwei Sun

Cite This: *ACS Omega* 2022, 7, 11722−11730

Read Online

ACCESS | Metrics & More | Article Recommendations | Supporting Information

**ABSTRACT:** Herein, we developed an efficient and convenient method to address the problem of thickener decomposition in the low- permeability oilfield production process. It is crucial to design breakers that reduce viscosity by delaying thickener decomposition in appropriate environments. By using lignin in biomass as a substrate for β-mannanase immobilization (MIL), we fabricated a gel breaker, surface gelatin-coated β-mannanase-immobilized lignin (Ge@MIL). Through experiments and performance tests, we confirmed that the prepared Ge@MIL can release enzymes at a specific temperature, meanwhile having temperature-sensitive phase change properties and biodegradability. The results also show the tight tuning over the surface coating of Ge@MIL by a water-in-oil emulsion. Therefore, the prepared Ge@MIL has a promising application in the field of oil extraction as a green and efficient temperature-sensitive sustained-release capsule.

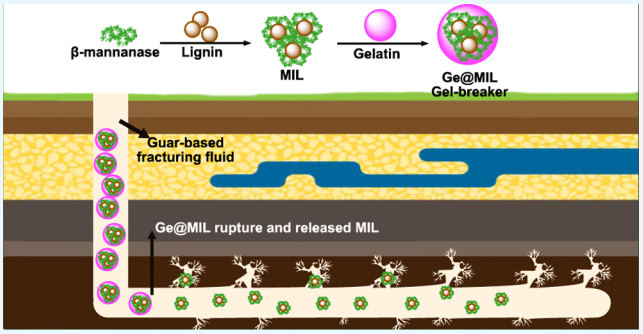


## 1. INTRODUCTION

Petroleum is a critical resource in the world, which is widely used in a variety of industries; with the increasing demand, more attention is being focused on the exploitation of low-permeability reservoirs.[1] The process involves fracturing, in which cracks are formed near the wellbore to improve oil recovery. The most common technique of fracturing is hydraulic fracturing.[2]

Thickeners and glue breakers are often applied in fracturing fluids. After the fracturing process is complete, the breaker reduces the viscosity of the thickener by destroying the structure of the thickener, so that the fracturing fluid can flow back smoothly.[3] However, almost no fracturing fluid is recovered at the end of the process, leaving a large amount of fluid deep in the formation.[4] The reason for that is the water-based fracturing fluid is injected into the oil well along with the breaker. As the breaker can only reduce the viscosity after completion of the fracturing process, the breaker needs to be equipped with the ability to release under certain conditions or delay its action on the thickener.[5] Otherwise, it will be difficult for the fracturing fluid to be recovered as backflow, which would remain underground and destroy the ecology of the underground.[6] Thus, designing breakers that reduce viscosity by delaying thickener decomposition in appropriate environments has become a useful tool to solve this challenge.

So far, guar gum has been commonly used as a thickener in hydraulic fracturing operations owing to its superior properties. The main chain of guar gum is composed of β-(1,4)-linked mannose, and its side chain is composed of α-(1,6)-linked galactose. After the fracturing process is complete, guar gum is destroyed by the breaker to form fractures. The degree of degradation of guar gum is affected by fracturing fluid discharge and permeability after fracturing, at the same time this also affects the fracturing fluid remaining underground and has an impact on the environment. Currently, the chemical breakers used to reduce the viscosity of fracturing fluid are potassium persulfate, ammonium persulfate, and other chemical reagents with strong oxidizing properties. However, the use of chemical reagents in the fracturing process has a number of disadvantages such as environmental pollution, insufficient strength for breaking the glue, and nonspecific chemical reactions, which limit their scope of application. In addition, the temperature of low-temperature oil wells (from 600 to 2300 ft) is often between 25.5 and 40.5 °C.[7] In this temperature range, the redox reaction activity is too slow and difficult to meet the requirements of rubber breaking.[8] Compared with chemical oxidants, enzyme breakers are attracting increasing interest for hydraulic fracturing systems. The β-mannanase enzyme breaker is a hemicellulose hydrolase.

**Received:** December 2, 2021
**Accepted:** March 17, 2022
**Published:** April 1, 2022

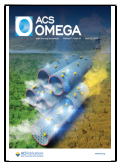

The 1,4-glycosidic bond in the structure of large mannan is broken by internal cutting, and the large and high viscosity mannan is hydrolyzed to the small and low viscosity mannan, so as to achieve the effect of gum breaking.[9] Compared with chemical oxidants, β-mannanase shows better reactivity at low temperatures, thus a β-mannanase gel breaker has great application prospects in low-temperature reservoirs. However, because the β-mannanase glue breaker is introduced at the same time as the fracturing fluid is injected into the oil pipeline, the function of the β-mannanase glue breaker can only be exerted under certain conditions.[10]

In this work, a green and simple method was developed for the fabrication of surface gelatin-coated β-mannanase-immobilized lignin (Ge@MIL) as a gel breaker that enables delayed release and enzyme activity stability of β-mannanase (Scheme 1). Ge@MIL synthesized in our study is distinguished by its temperature sensitivity, enzyme immobilization, and complete biodegradability. To provide Ge@MIL with stable and high enzyme activity, we used lignin in biomass as a substrate for β-mannanase immobilization.[11] The synthesis method was based on batch processing techniques; therefore, it can be produced on a large scale. In addition, we explored an efficient and convenient method that led to tight tuning over the surface coating of Ge@MIL by water-in-oil (w/o) emulsion. It is worth mentioning that the surface coating material we used has temperature-sensitive phase change properties and biodegradability.[12] More and more researchers have paid attention to gelatin temperature-sensitive sustained-release materials.[13−16]

Finally, we demonstrate that the prepared Ge@MIL can release enzymes at a specific temperature while rapidly degrading guar gum and reducing its viscosity, and it is an excellent breaker with delayed release functions. Ge@MIL has great application prospects in the field of temperature-sensitive sustained release.

**Scheme 1. Illustration of Surface Gelatin-Coated β-Mannanase-Immobilized Lignin (Ge@MIL)**

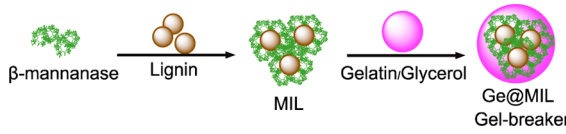


## 2. RESULTS AND DISCUSSION

**2.1. Characterization of Free and Immobilized β-Mannanase.** The characteristic functional groups of β-mannanase and lignin nanoparticles were found in the FT-IR spectrum of MIL, which confirmed the success of MIL preparation. As shown in Figure 1a, the immobilization resulted in a strong characteristic peak of MIL at 2900−3042 $cm^{-1}$, and the vibration peak is ascribed to the interaction of O−H and N−H groups in β-mannanase and the C−H stretching vibrations in aromatic methoxyl groups absorption peak of lignin.[24] The position of the vibration absorption peak will shift forward. The vibrational peak at 1657 $cm^{-1}$, which is ascribed to the N−H stretching vibration in the enzyme, is shifted to 1641 $cm^{-1}$ in the MIL. This is attributed to the fact that the enzyme is mainly covalently linked to the matrix or physical partial immobilization.

The SEM images revealed that the prepared lignin nanoparticles exhibit an average size of 100 ± 20 nm (Figure 1b), and a small fraction of spherical-like grains is also observed. As shown in Figure 1c, the MIL changes the morphology of lignin and makes it more aggregated and hydrophobic due to H bonding and interaction between lignin and the β-mannanase enzyme. Phenolic hydroxyl groups in the structure of lignin play a key role in the interaction between lignin and enzymes.[25] SEM revealed that both lignin and MIL were dispersed in the structure and had clear and complete structures. An EDS analyzer was used to determine the difference in the elemental composition of the prepared lignin nanoparticle and MIL. As compared to lignin nanoparticles (Figure 1b), MIL contains the N element in addition to C and O elements. This result indicated that β-mannanase was successfully immobilized onto lignin nanoparticles because the N element is a constituent element of β-mannanase and not lignin.

**2.2. Preparation and Optimization of β-Mannanase Immobilization onto Lignin.** Figure 2a,b shows that the quantity of the immobilized β-mannanase increases with increasing process duration and concentration of the enzyme solution. The maximum relative activity of the enzyme was 87% at 80 min and 3 mg/mL, and the loading of enzymes was 22.2 mg/g. The trends between the amount of immobilized enzymes and enzyme activity were analyzed to demonstrate that the diffusive transport of the substrate to the attached enzyme was greatly enhanced during the reaction.[26] The amount of immobilized peptide increased by extending the

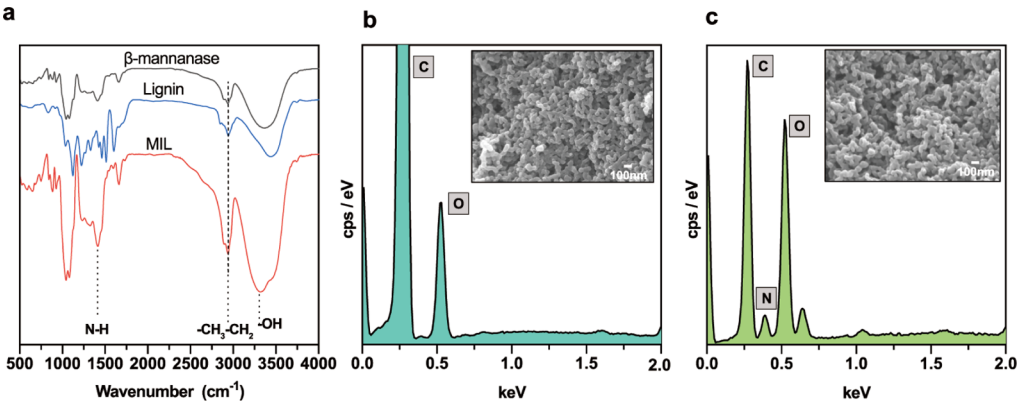


**Figure 1.** Structural characterization of MIL. (a) FTIR spectrum of MIL, (b) EDS spectrum and SEM image of lignin, and (c) EDS spectrum and SEM image of MIL.



https://doi.org/10.1021/acsomega.1c06817
ACS Omega 2022, 7, 11722−11730

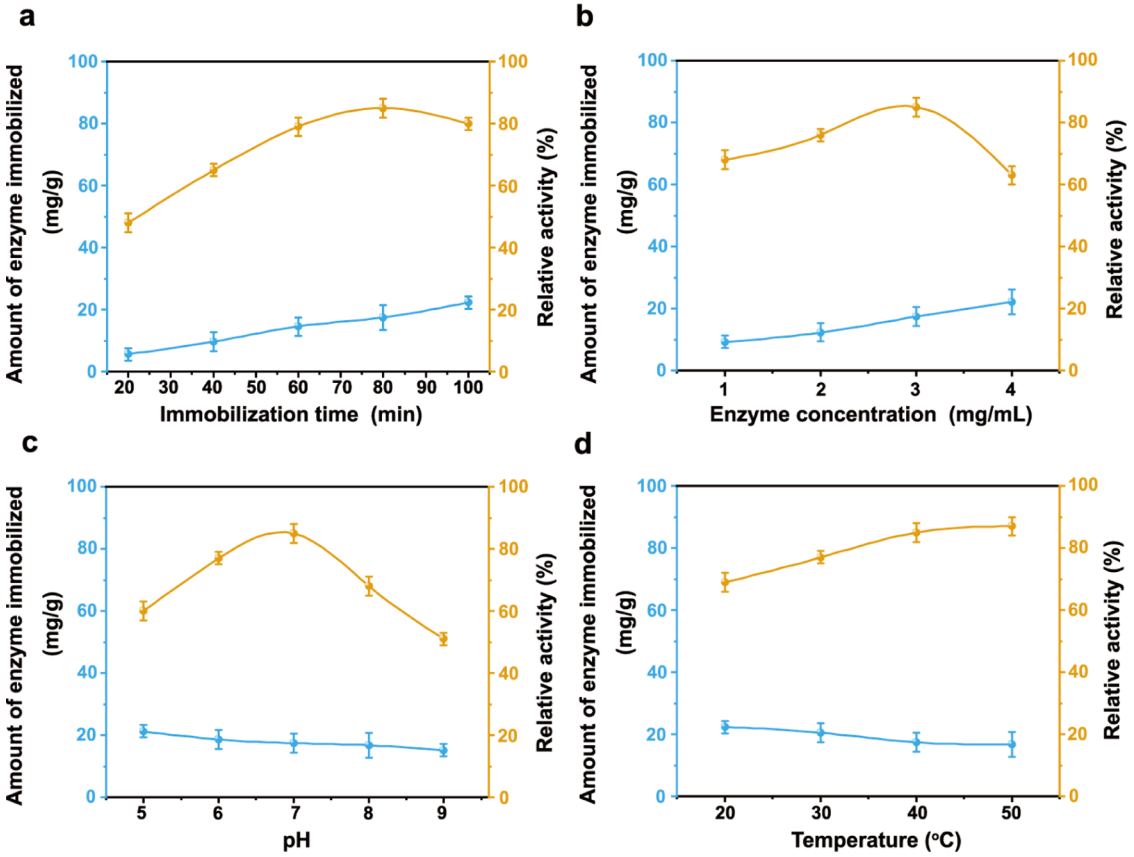


**Figure 2.** Effect of immobilization conditions on the amount of immobilized enzyme and relative activity of immobilized enzyme (a) Immobilization time, (b) enzyme concentration, (c) pH, and (d) temperature. The yellow line is the relative activity and the blue line is the amount of immobilized enzymes. Error bars represent standard deviation ($n$ = 3) for each data point.

time of immobilization of the enzyme (100 min) and increasing the initial amount of the enzyme (4 mg/g), but the enzyme activity decreased. This is owing to the high hydrophobicity of lignin inhibiting the activity of enzymes.[27]

The influence of pH on buffer during immobilization was also investigated. As can be seen from the blue line in Figure 2c, the maximum enzyme loading (21 mg/g) was reached at pH 5, resulting from the protonation of the OH group on the surface of the hybrid group. The protonation of the group will attract a large number of negatively charged $\beta$-mannanase particles and therefore, the amount of immobilized enzymes will increase. As the group does not protonate in an alkaline environment, the amount of immobilized enzymes is less, and the activity of enzymes is also relatively less, owing to the separation of some amino acids in the structure.[28] Under the optimum conditions (pH = 7, 40 °C), the structure of the peptide does not change. With increasing temperature, a slight decrease in the relative activity is observed, which is related to the partial thermal inactivation of the peptide, while there is a slight increase in the quantity of bound enzymes.[29]

**2.3. Gelatin-Coated $\beta$-Mannanase-Immobilized Lignin (Ge@MIL).** In the process of guar-based fracturing fluid oil recovery, it is required that guar gum not be degraded before reaching the oil production point. Therefore, it is necessary to prevent $\beta$-mannanase enzymes from degrading guar gum during transportation.[30] Therefore, in this work, a gelatin-coated $\beta$-mannanase-immobilized lignin (Ge@MIL) was reported.

To investigate the encapsulation efficiency of the immobilized enzyme, the different conditions of temperature, concentration of gelatin, stirring rate, and MIL/gelatin (wt/wt) were investigated (Figure 3a–d). It was observed that the encapsulation efficiency of the immobilized enzyme slowly increased at the temperature from 20 to 50 °C in Figure 3a. At 50 °C, the encapsulation efficiency reached a maximum of 87%. The results clearly showed that the increase of the temperature will accelerate the speed of the chemical reaction and improve the efficiency of the chemical reaction, and the encapsulation efficiency of the immobilized enzyme was also enhanced. However, when the temperature was increased to 60 °C, the structure of the enzyme will be broken, resulting in the decrease of the encapsulation efficiency of the immobilized enzyme.[31] As shown in Figure 3b, with the increase of the gelatin concentration (from 10 to 25%), the encapsulation efficiency of immobilized enzymes showed a decreasing trend. When the gelatin concentration was 10%, the encapsulation efficiency of the immobilized enzyme was the highest. The effect of the stirring rate of the immobilized enzyme used in the encapsulation efficiency. As can be seen in Figure 3c, when the stirring speed is at the ranges of 450 to 650 rpm the encapsulation efficiency of the immobilized enzyme increased, the highest encapsulation efficiency of 89.2% was achieved at 650 rpm. However, when the stirring speed is at the ranges of 650 to 750 rpm, the Ge@MIL will be broken and the encapsulation efficiency of the immobilized enzyme will decrease.[32] As shown in Figure 3d, with the reduction of MIL/gelatin (wt/wt), the encapsulation efficiency presents a


https://doi.org/10.1021/acsomega.1c06817
ACS Omega 2022, 7, 11722−11730

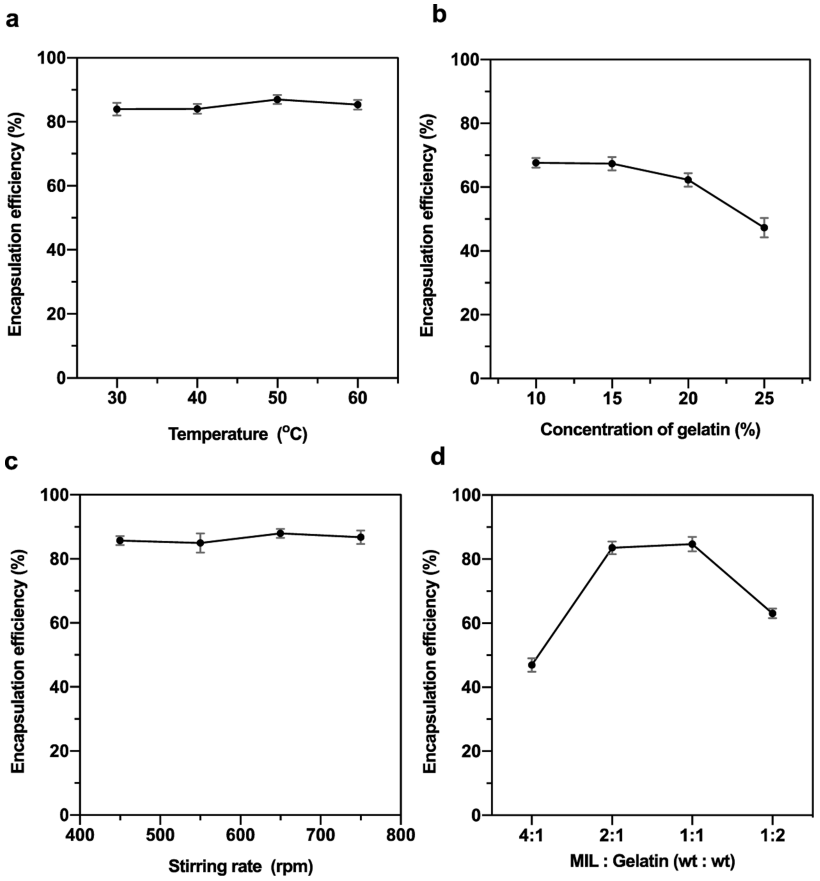


**Figure 3.** Effect of encapsulation conditions on the encapsulation efficiency. (a) Temperature, (b) concentration of gelatin, (c) stirring rate, and (d) MIL/gelatin (wt/wt). Error bars represent standard deviation ($n$ = 3) for each data point.

rapid rise (4:1 to 2:1) first, then slowly rises (2:1 to 1:1), and finally drops (1:1 to 1:2), when a MIL/gelatin (wt/wt) of 1:1, the encapsulation efficiency is maximum up to 82%.[33]

**2.4. Morphology, Pressure-Resistant Properties, and Phase-Transition Performance of Ge@MIL.** The surface morphology, pressure-resistant properties, and phase transition performance of Ge@MIL were analyzed using SEM, EDS, universal material testing machine, and DSC, and the results are presented in Figure 4a−e. The SEM of Ge@MIL with different concentrations of gelatin emulsification temperature and stirring speed is shown in Figures 4a and S1 and S2, respectively. The result indicated that the Ge@MIL id roughly spherical in shape with an average size in the narrow range of 60−70 $\mu$m. When the gelatin concentration was 10% (10% Ge@MIL), the coating effect of gelatin on MIL was poor, and it was difficult to form a spherical shape. As the concentration of gelatin increases, the coating effect becomes more uniform and tends to be spherical. A morphology of 20% Ge@MIL (20% gelatin) is more complete and the microspheres are not fractured or condensed.[34] To better determine the coating relationship between gelatin and MIL, 20% Ge@MIL and section of 20% Ge@MIL (fractured under liquid nitrogen) were stained with 1% $KMnO_4$ for 10 min to selectively stain for lignin before EDS mapping analysis, the results shown in Figure 4b,c. As shown in Figure 4b, the surface of the 20% Ge@MIL sphere was mainly composed of C, O, and N elements, while Mn elements were basically absent. This shows that there was basically no MIL on the surface of the 20% Ge@MIL sphere. After being fractured under liquid nitrogen (Figure 4c), the Mn elements were marked uniformly on the inner structure of the section of 20% Ge@MIL. These results indicated that the MIL was completely coated inside the gelatin ball during the gelatin coating process, which would help limit the premature biodegradation of the gum by MIL during the transportation process.[35]

In practical oil recovery applications of guar-based fracturing fluid, Ge@MIL is generally required to have a certain environmental pressure tolerance.[36] Glycerol (Gly) as a plasticizer was employed to improve the pressure-resistant properties of Ge@MIL during the preparation process. The pressure-resistant properties of Ge@MIL obtained with different concentrations of Gly is shown in Figure 4d. When the concentration of Gly increased from 10 to 25%, the pressure resistance of the prepared Ge@MIL could all meet the tolerance requirements of practical applications. With the decrease of the glycerol content, the hardness of the Ge@MIL will gradually increase the deformation degree will decrease under the same pressure, and the pressure resistance of the Ge@MIL shows an upward trend.[37]

Additionally, the temperature of low-temperature hydrocarbon reservoirs (2300 ft) is about 40 °C. This requires MIL to be able to produce a good phase change at about 40 °C to release the MIL encapsulated in the Ge@MIL. The temperature-sensitive performance of the Ge@MIL obtained with different concentrations of Gly is shown in Figure 4e. When the temperature was between 20 and 40 °C, the degree of phase transformation did not occur in all samples. At a concentration of Gly of 0%, the sample produces a phase


https://doi.org/10.1021/acsomega.1c06817
ACS Omega 2022, 7, 11722−11730

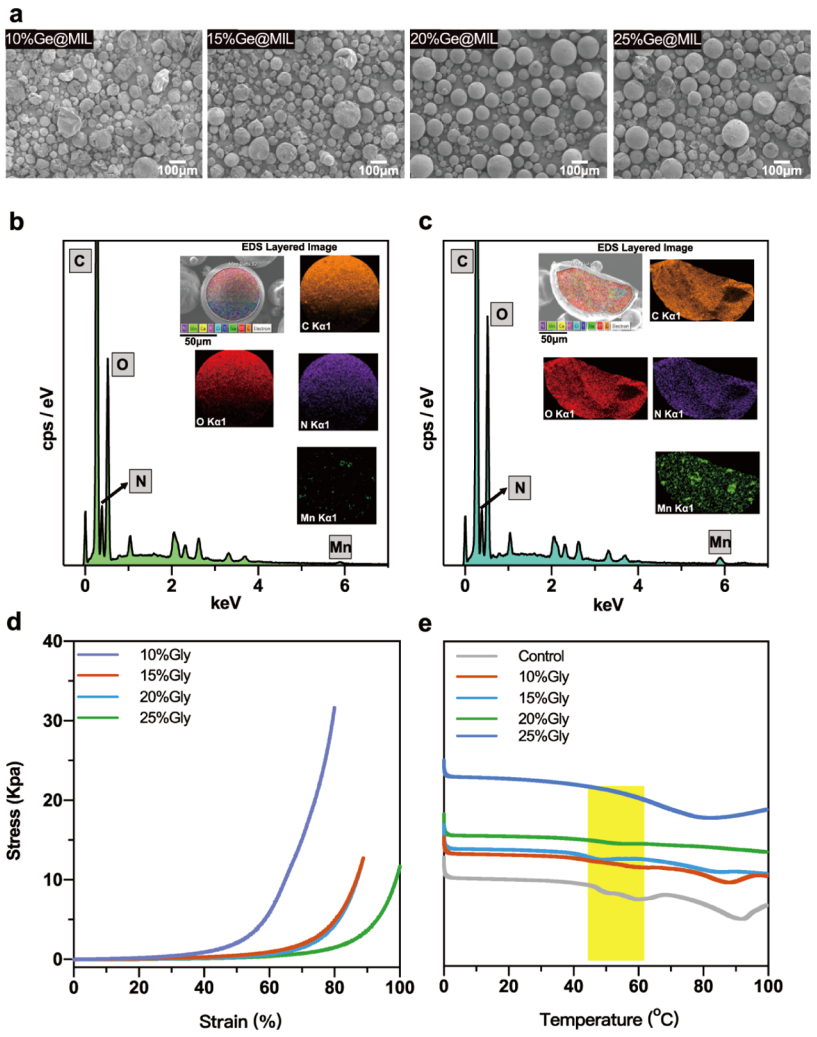


**Figure 4.** Surface morphology, pressure resistance, and phase transition performance of Ge@MIL. (a) SEM images, (b) EDS mapping of 20% Ge@MIL, (c) EDS mapping of 20% Ge@MIL section, (d) pressure-resistant properties, and (e) DSC curves of Ge@MIL.

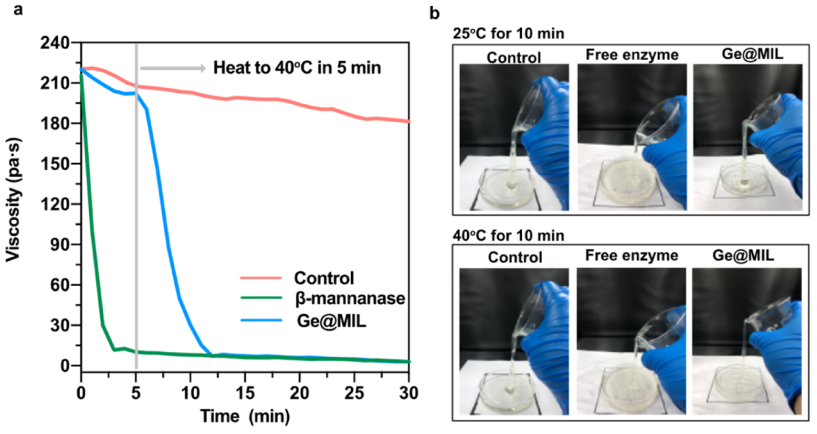


**Figure 5.** Viscosity curve (a) and apparent viscosity (b) of the guar-based fracturing fluid by free $\beta$-mannanase and Ge@MIL.

change at 45−60 °C. The long phase transition temperature range was not conducive to the rapid release of MIL from Ge@MIL. With the increase of the concentration of Gly, the phase transition temperature of the Ge@MIL decreased slightly, which shows that the introduction of Gly was able to improve the shell pressure resistance without negatively affecting the phase change temperature of the Ge@MIL shell. When the concentration of Gly increased to 15%, the phase transition temperature was 42.2 °C. This phenomenon was conducive to the rapid phase change of Ge@MIL after entering the crust, and the rapid release of MIL from Ge@MIL to biodegrade the guar gum.[38]

**2.5. Application of Free Laccase and Ge@MIL for Guar-Based Fracturing Fluid.** Guar gum is widely used as a



https://doi.org/10.1021/acsomega.1c06817
ACS Omega 2022, 7, 11722−11730

thickening agent in fracturing fluids, which is difficult to degrade in natural environments after flowing back to the ground and has caused great harm to the environment. To meet the allowable discharge standards, that is, a fracturing fluid viscosity of less than 5 pa*s, an enzyme-based gel breaker is used to remove the guar gum residue to reduce its viscosity to repair reservoir fracturing fluid damage. The temperature of low-temperature hydrocarbon reservoirs (2300 ft) is about 40 °C.[39] Therefore, the breaker needs almost no contact with the guar fracturing fluid, which allows the fracturing fluid to maintain high viscosity as it enters the oil well. Meanwhile, the gel breaker can quickly degrade guar-based fracturing fluids after reaching the reservoirs, thereby reducing the viscosity, and subsequently promoting backflow.[40] The effect of the free enzyme and the Ge@MIL on reducing viscosity of the guar-based fracturing fluid was measured at 25 and 40 °C (Figure 5). As shown in Figure 5a, Ge@MIL had a great effect on delaying the viscosity reduction of fracturing fluid as compared to free β-mannanase at 25 °C (before 5 min). Afterward, the samples were heated to 40 °C at 5 min, Ge@MIL produced phase transition and rupture and released the MIL, then the guar-based fracturing fluid was biodegraded by the MIL and caused the viscosity of fracturing fluid to gradually decrease. After 10 min, the viscosity of fracturing fluid was reduced to the allowable emission standard (5 Pa*s) in 12 min (Figure 5a). Figure 5b shows the apparent viscosity, after the samples were maintained at room temperature for 10 min, the viscosity of guar-based fracturing fluid with Ge@MIL was similar to that of the control group. However, the viscosity of guar-based fracturing fluid with free β-mannanase had decreased rapidly as compared to the control and Ge@MIL groups. After the samples were maintained at 40 °C for 10 min, the viscosity of the guar-based fracturing fluid with Ge@MIL was similar to that of the free β-mannanase group. The apparent viscosity and viscosity curve of the guar-based fracturing fluid indicated that the Ge@MIL has a good adhesive breaking effect in low-temperature reservoirs below 40 °C.[41] In addition, the salinity tolerance of Ge@MIL was also tested. Ge@MIL was immersed in saturated NaCl aqueous solution for 480 min and the stability of Ge@MIL was observed by optical microscopy. Figure S3 shows that Ge@MIL retains its morphological integrity even after 480 min of immersion in saturated NaCl aqueous solution, indicating its high salt-resistance.

## 3. CONCLUSIONS

We introduced a truly effective synthetic method to address the problem that thickener decomposition in low-permeability oilfield production processes, in which by using lignin in biomass as a substrate for β-mannanase immobilization (MIL) and surface gelatin-coated β-mannanase-immobilized lignin (Ge@MIL). The SEM displayed that Ge@MIL is spherical in shape with an average size in the narrow range of 60−70 μm, the morphology of 20% Ge@MIL (20% gelatin) was more complete, the particles were more dispersed, and the surface has no fracture and no condensation was observed. Moreover, we successfully demonstrated that the MIL was completely coated inside the gelatin ball during the gelatin coating process, thanks to these unique properties which would help limit the premature biodegradation of the gum by MIL during the transportation process. These characteristics highlight that we demonstrate that the prepared Ge@MIL can release enzymes at a specific temperature while rapidly degrading guar gum and reducing its viscosity, it is an excellent breaker with delayed release functions. It has broad application prospects in low-permeability oilfields.

## 4. EXPERIMENTAL SECTION

**4.1. Materials and Chemicals.** Ethanol lignin was prepared from hybrid poplar by an organic solvent ethanol method. Gelatin (type B, BC; ∼250 Bloom, $M_w$ = 100 kDa), glycerol (Gly), and acetone were purchased from Aladdin Inc. Guar gum (over 99.99% purity) was obtained from Chengdu Aike Reagent Co., Ltd. Coomassie Brilliant Blue G-250 (CBB G-250) dye, 3,5-dinitrosalicylic acid (DNS), and bovine serum albumin (BSA) were obtained from Sigma-Aldrich. All reagents used in this work were of analytical grade and used without further purification.

**4.2. Preparation of β-Mannanase Immobilization onto Lignin Nanoparticles.** Lignin nanoparticles were prepared by diluting the stock solution with ethanol organic solvent according to Lv et al.[17] For the immobilization of the β-mannanase enzyme onto lignin nanoparticles, 50 mg of lignin nanoparticles was used and 10 mL of the β-mannanase enzyme solution in buffer at appropriate pH (from 5 to 9), at a concentration in the range from 1 to 4 mg/mL, was added. The mixture was placed in a constant temperature shaker and was shaken for a specified period of time varying from 20 to 100 min at a temperature ranging from 20 to 50 °C. The immobilized β-mannanase enzyme was then centrifuged and washed three times with the same buffer solution. The immobilized enzyme was then stored at 4 °C in the same buffer until further use. The β-mannanase activity bound (MAB) onto MIL is estimated from eq 1[18]

$$\mathrm{MAB}\ (\%) = 100 \times [\mathrm{MA_i} - (\mathrm{MA_s} + \mathrm{MA_w})]/\mathrm{MA_i} \quad (1)$$

where $MA_i$ is the β-mannanase activity added, $MA_s$ is the β-mannanase activity measured in the supernatant after the collection of MIL, and $MA_w$ is the β-mannanase activity measured in the pooled washing fractions.

**4.3. Surface Gelatin-Coated β-Mannanase-Immobilized Lignin (Ge@MIL).** 1−2.5 g of gelatin was dissolved in 10 g of water (concentration ranges 10−25%) at 60 °C under stirring for 1 h to form the GEL solution. Based on the gelatin content in the GEL solution, different quantities of MIL solution were added dropwise to achieve final MIL/gelation molar ratios of 4:1, 2:1, 1:1, and 1:2, while stirring at 450−750 rpm with a mechanical stirrer to form the GEL−MIL solution. Glycerol (Gly) was added as a plasticizer to the GEL−MIL solution at a concentration of 10−25% (w/w dry gelatin matter) and the GEL/MIL solutions were maintained under stirring for 30 min. Then, the GEL−MIL solution was added dropwise into 60 mL of olive oil at 30−60 °C, while stirring at 450−750 rpm with a mechanical stirrer. The water-in-oil (w/o) emulsion was stirred for 10 min before being immersed into an ice bath to maintain the temperature at 10 °C and stirred for a further 30 min. The precipitates were redispersed in 12 mL of deionized water with brief sonication and dialyzed against deionized water overnight. The surface gelatin-coated β-mannanase-immobilized lignin (Ge@MIL) was collected by removing deionized water by centrifugation and air dried.[19]

**4.4. Assay of Free and Immobilized β-Mannanase Activity.** The activities of free and lignin-immobilized β-mannanase were determined by using the DNS method by measuring the amount of reducing sugar released from LBG according to the method described by Mohapatra. Briefly, the standard mixture determination is required to contain of 0.1



https://doi.org/10.1021/acsomega.1c06817
ACS Omega 2022, 7, 11722−11730

mL of free or immobilized $\beta$-mannanase preparation, 0.4 mL of 50 mmol/L Trizma buffer (pH 7.5), and 0.5 mL of 1% of LBG resuspended in the same buffer. The sample to be tested was placed in warm water at 50 °C for 30 min. The absorbance was measured at 540 nm. One unit of enzyme is defined as the amount that liberated 1 $\mu$mol of mannose sugar per minute under the assay conditions. Values were expressed as mean ± S.D. One-way analysis of variance (ANOVA) was performed on all the experimental measurements. Data were compared by the least significant difference (LSD) or the Duncan's multiple range test.

**4.5. Characterization of MIL and Ge@MIL.** The quantity of $\beta$-mannanase immobilized on the surface of lignin was determined based on the Bradford method by measuring the initial and final quantities of $\beta$-mannanase in the immobilization medium.[20] Bsa solution at known concentrations was calibrated to calculate binding levels. The encapsulation efficiency (EE) of gelatin for MIL was determined using the following eq 2

$$EE = (Q_{MIL}/Q_{total})100 \quad (2)$$

where EE is the percentage encapsulation of the Ge@MIL, $Q_{MIL}$ is the quantity of MIL encapsulated in Ge@MIL (g), and $Q_{total}$ is the quantity of MIL added for encapsulation (g).

The functional group analysis of the free and immobilized $\beta$-mannanase was done using Fourier transform-infrared spectroscopy (FT-IR, Thermo Nicolet, ModelAvatar 370, USA). The scanning range of FT-IR spectrum is 400−4000 $cm^{-1}$. The morphology and elemental composition of the MIL, Ge@MIL, and Ge@MIL sections was observed under scanning electron microscopy (SEM) in combination with energy-dispersive X-ray spectrometry (EDS) with a JEOL JSM-5800 model. To better determine the coating relationship between gelatin and MIL, Ge@MIL and Ge@MIL sections (fractured under liquid nitrogen) were stained with 1% $KMnO_4$ for 10 min to selectively stain the lignin before EDS analysis. Granule pressure-resistant properties of Ge@MIL was performed on an universal material testing machine (INSTRON5960, Norwood, MA, USA) and parameter registration by the computer system "Bluehill". The test sample was 15 mm in diameter and 5 mm thick. Prior to the test, the samples were ground to obtain flat faces for uniform load transfer. This is followed by applying compressive load through two diametrically opposite rigid platens.[21]

**4.6. Application of Free $\beta$-Mannanase and Ge@MIL for Guar-Based Fracturing Fluid.** The breaking effect of the glue breaker was evaluated by the change of apparent viscosity.[22] Refer to "Methods for the Performance Evaluation of Water-based Fracturing Fluid" (SY/T 5107-2005) for the fracturing fluid preparation method.[23] The viscosity of the sample to be tested is measured by a rotary viscometer (Brookfield Engineering Labs., Middleboro, MA, USA). The sample (100 mL) was added in a circular cylindrical container with a rotation rate of 60 rpm.

## ■ ASSOCIATED CONTENT

### Supporting Information

The Supporting Information is available free of charge at https://pubs.acs.org/doi/10.1021/acsomega.1c06817.

SEM analysis and optical microscopy salinity tolerance test of Ge@MIL (PDF)

## ■ AUTHOR INFORMATION


### Corresponding Authors

**Xing Wang** − *Liaoning Key Lab of Lignocellulose Chemistry and BioMaterials, Liaoning Collaborative Innovation Center for Lignocellulosic Biorefinery, College of Light Industry and Chemical Engineering, Dalian Polytechnic University, Dalian 116034, China;* orcid.org/0000-0002-1539-5741; Phone: +86-411-86323736; Email: wangxing@dlpu.edu.cn

**Ying Han** − *Liaoning Key Lab of Lignocellulose Chemistry and BioMaterials, Liaoning Collaborative Innovation Center for Lignocellulosic Biorefinery, College of Light Industry and Chemical Engineering, Dalian Polytechnic University, Dalian 116034, China;* orcid.org/0000-0002-0213-8412; Email: hanying@dlpu.edu.cn

### Authors

**Haonan Cong** − *Liaoning Key Lab of Lignocellulose Chemistry and BioMaterials, Liaoning Collaborative Innovation Center for Lignocellulosic Biorefinery, College of Light Industry and Chemical Engineering, Dalian Polytechnic University, Dalian 116034, China*

**Zihao Ma** − *Liaoning Key Lab of Lignocellulose Chemistry and BioMaterials, Liaoning Collaborative Innovation Center for Lignocellulosic Biorefinery, College of Light Industry and Chemical Engineering, Dalian Polytechnic University, Dalian 116034, China*

**Meixi Hu** − *Liaoning Key Lab of Lignocellulose Chemistry and BioMaterials, Liaoning Collaborative Innovation Center for Lignocellulosic Biorefinery, College of Light Industry and Chemical Engineering, Dalian Polytechnic University, Dalian 116034, China*

**Junjie Han** − *Department of Research and Development, Dalian Chivy Biotechnology CO., LTD., Dalian 116034, China*

**Yao Li** − *Liaoning Key Lab of Lignocellulose Chemistry and BioMaterials, Liaoning Collaborative Innovation Center for Lignocellulosic Biorefinery, College of Light Industry and Chemical Engineering, Dalian Polytechnic University, Dalian 116034, China;* orcid.org/0000-0003-4784-2785

**Guangwei Sun** − *Liaoning Key Lab of Lignocellulose Chemistry and BioMaterials, Liaoning Collaborative Innovation Center for Lignocellulosic Biorefinery, College of Light Industry and Chemical Engineering, Dalian Polytechnic University, Dalian 116034, China*

Complete contact information is available at: https://pubs.acs.org/10.1021/acsomega.1c06817


### Notes

The authors declare no competing financial interest.

## ■ ACKNOWLEDGMENTS

This research was funded by the National Natural Science Foundation of China (nos. 21908014), Liaoning Education Department Project (no. J2020038), Liaoning University Innovation Talent Program in 2020, the Special Financial grant from the China Postdoctoral Science Foundation (no. 2020T130464), and the Foundation of Guangxi Key Laboratory of Clean Pulp & Papermaking and Pollution Control, College of Light Industry and Food Engineering, Guangxi University (no. 2021KF01).

## REFERENCES


(1) Cai, W. B.; Qin, G. W.; An, Y. F.; Zhang, Y. L. Study on Horizontal Well Fracture in Low Permeability Reservoirs. *Adv. Mater.* **2012**, *524*−*527*, 1587−1590.

(2) Barati, R.; Liang, J.-T. A review of fracturing fluid systems used for hydraulic fracturing of oil and gas wells. *Appl. Polym. Symp.* **2014**, *131*, 40735−40746.

(3) Brannon, H. D.; Pulsinelli, R. J. Breaker Concentrations Required To Improve The Permeability Of Proppant-Packs Damaged By Concentrated Linear And Borate-Crosslinked Fracturing Fluids. *J. Pet. Sci. Eng.* **1990**, *7*, 338−342.

(4) Lester, Y.; Yacob, T.; Morrissey, I.; Linden, K. G. Can We Treat Hydraulic Fracturing Flowback with a Conventional Biological Process. The Case of Guar Gum. *Environ. Sci. Technol. Lett.* **2013**, *1*, 133−136.

(5) Hu, K.; Li, C.-X.; Pan, J.; Ni, Y.; Zhang, X.-Y.; Xu, J.-H. Performance of a New Thermostable Mannanase in Breaking Guar-Based Fracturing Fluids at High Temperatures with Little Premature Degradation. *Appl. Biochem. Biotechnol.* **2013**, *172*, 1215−1226.

(6) Meller, C.; Kohl, T. The significance of hydrothermal alteration zones for the mechanical behavior of a geothermal reservoir. *Geotherm. Energy.* **2014**, *2*, 2−21.

(7) Wu, F.-p.; Liu, J.; Wei, X.-m.; Pu, C.-s. A study on oxygen consumption mechanism of air-foam flooding in low-temperature oil reservoir. *J. Pet. Sci. Eng.* **2018**, *161*, 368−380.

(8) Chuanliang, Y.; Yuanfang, C.; Ji, T.; Guojin, Z.; Zhongchao, Y.; Yuwen, L.; Fucheng, D. The influence of steam stimulation on compression coefficient of heavy oil reservoirs. *J. Pet. Explor. Prod. Technol.* **2017**, *8*, 1287−1294.

(9) Chen, J.; Eraghi Kazzaz, A.; AlipoorMazandarani, N.; Hosseinpour Feizi, Z.; Fatehi, P. Production of Flocculants, Adsorbents, and Dispersants from Lignin. *Molecules* **2018**, *23*, 868−893.

(10) Lv, L.; Lin, J.; Feng, Y.; Wang, W.; Li, S. Coated recombinant Escherichia coli for delayed release of $\beta$-mannanase in the water-based fracturing fluid. *Process Biochem.* **2021**, *107*, 121−128.

(11) Mohapatra, B. R. Characterization of $\beta$-mannanase extracted from a novel Streptomyces species Alg-S25 immobilized on chitosan nanoparticles. *Biotechnol. Biotechnol. Equip.* **2021**, *35*, 150−161.

(12) He, Y.; Li, W.; Han, N.; Wang, J.; Zhang, X. Facile flexible reversible thermochromic membranes based on micro/nanoencapsulated phase change materials for wearable temperature sensor. *Appl. Energy* **2019**, *247*, 615−629.

(13) Aydin, N. E. Effect of Temperature on Drug Release: Production of 5-FU-Encapsulated Hydroxyapatite-Gelatin Polymer Composites via Spray Drying and Analysis of In Vitro Kinetics. *Int. J. Polym. Sci.* **2020**, *2020*, 1−13.

(14) Suarasan, S.; Focsan, M.; Potara, M.; Soritau, O.; Florea, A.; Maniu, D.; Astilean, S. Doxorubicin-Incorporated Nanotherapeutic Delivery System Based on Gelatin-Coated Gold Nanoparticles: Formulation, Drug Release, and Multimodal Imaging of Cellular Internalization. *ACS Appl. Mater. Interfaces* **2016**, *8*, 22900−22913.

(15) Park, K.-S.; Kim, C.; Nam, J.-O.; Kang, S.-M.; Lee, C.-S. Synthesis and characterization of thermosensitive gelatin hydrogel microspheres in a microfluidic system. *Macromol. Res.* **2016**, *24*, 529−536.

(16) Cheng, Y.-H.; Hung, K.-H.; Tsai, T.-H.; Lee, C.-J.; Ku, R.-Y.; Chiu, A. W.-h.; Chiou, S.-H.; Liu, C. J.-l. Sustained delivery of latanoprost by thermosensitive chitosan-gelatin-based hydrogel for controlling ocular hypertension. *Acta Biomater.* **2014**, *10*, 4360−4366.

(17) Lv, J.; Christie, P.; Zhang, S. Uptake, translocation, and transformation of metal-based nanoparticles in plants: recent advances and methodological challenges. *Environ. Sci.: Nano* **2019**, *6*, 41−59.

(18) Ahmed, A. Y.; Aowda, S. A.; Hadwan, M. H. A validated method to assess glutathione peroxidase enzyme activity. *Chem. Pap.* **2021**, *75*, 6625−6637.

(19) Dai, L.; Liu, R.; Hu, L.-Q.; Zou, Z.-F.; Si, C.-L. Lignin Nanoparticle as a Novel Green Carrier for the Efficient Delivery of Resveratrol. *ACS Sustainable Chem. Eng.* **2017**, *5*, 8241−8249.

(20) Al-Shams, J. K. J.; Hussein, M. A.; A-Hakeim, H. K. Activity and stability of urease enzyme immobilized on Amberlite resin. *Ovidius Univ. Ann. Chem.* **2020**, *31*, 1−4.

(21) Mieldazys, R.; Jotautiene, E.; Zinkeviciene, R.; Jasinskas, A. Manure processing into granular fertilizers using additional additives. *Dev* **2019**, *5*, 22−24.

(22) Soe, A. K.; Azahar, B. S. B. N.; Tunio, S. Q. Fracturing Fluid (Guar Polymer Gel) Degradation Study by using Oxidative and Enzyme Breaker. *Res. J. Appl. Sci. Eng. Technol.* **2012**, *4*, 1667−1671.

(23) Wei, X.-B.; Li, X.-R.; Wang, L.; Wang, X.-R.; Ma, G.-Y. Laboratory Evaluation and Field Application of a Type of Polyhydric Alcohols Fracturing Fluid. *J. Technol.* **2013**, *12*, 7789−7795.

(24) Yu, M.; He, D.; Zhang, Y.; He, D.; Wang, X.; Zhou, J. Characterization of lignin extracted from Acanthopanax senticosus residue using different methods on UV-resistant behavior. *Int. J. Biol. Macromol.* **2021**, *192*, 498−505.

(25) Zhao, X.; Meng, X.; Ragauskas, A. J.; Lai, C.; Ling, Z.; Huang, C.; Yong, Q. Unlocking the secret of lignin-enzyme interactions: Recent advances in developing state-of-the-art analytical techniques. *Biotechnol. Adv.* **2021**, *54*, 107830.

(26) Sharma, A.; Sood, K.; Kaur, J.; Khatri, M. Agrochemical loaded biocompatible chitosan nanoparticles for insect pest management. *Biocatal. Agric. Biotechnol.* **2019**, *18*, 101079.

(27) Chen, Y.; Liu, Y.; Li, X.; Zhang, J.; Li, G. Lignin Interacting with a-glucosidase and its Inhibitory Effect on the Enzymatic Activity. *Food Biophys.* **2015**, *10*, 264−272.

(28) Zimniewska, M. Functionalization of Natural Fibres Textiles by Improvement of Nanoparticles Fixation on Their Surface. *Bioeng* **2012**, *5*, 321−339.

(29) Espinoza-Acosta, J. L.; Torres-Chávez, P. I.; Olmedo-Martínez, J. L.; Vega-Rios, A.; Flores-Gallardo, S.; Zaragoza-Contreras, E. A. Lignin in storage and renewable energy applications: A review. *J. Energy Chem.* **2018**, *27*, 1422−1438.

(30) Vukoje, M.; Miljanić, S.; Hrenović, J.; Rožić, M. Thermochromic ink−paper interactions and their role in biodegradation of UV curable prints. *Cellulose* **2018**, *25*, 6121−6138.

(31) Piccinino, D.; Capecchi, E.; Botta, L.; Bizzarri, B. M.; Bollella, P.; Antiochia, R.; Saladino, R. Layer-by-Layer Preparation of Microcapsules and Nanocapsules of Mixed Polyphenols with High Antioxidant and UV-Shielding Properties. *Biomacromolecules* **2018**, *19*, 3883−3893.

(32) Sipponen, M. H.; Farooq, M.; Koivisto, J.; Pellis, A.; Seitsonen, J.; Österberg, M. Spatially confined lignin nanospheres for biocatalytic ester synthesis in aqueous media. *Nat. Commun.* **2018**, *9*, 2300−2309.

(33) Capecchi, E.; Piccinino, D.; Delfino, I.; Bollella, P.; Antiochia, R.; Saladino, R. Functionalized Tyrosinase-Lignin Nanoparticles as Sustainable Catalysts for the Oxidation of Phenols. *Nanomater* **2018**, *8*, 438−455.

(34) Mattinen, M.-L.; Valle-Delgado, J. J.; Leskinen, T.; Anttila, T.; Riviere, G.; Sipponen, M.; Paananen, A.; Lintinen, K.; Kostiainen, M.; Österberg, M. Enzymatically and chemically oxidized lignin nanoparticles for biomaterial applications. *Enzyme Microb. Technol.* **2018**, *111*, 48−56.

(35) Xiao, M.; Chen, W.; Li, W.; Zhao, J.; Hong, Y.-l.; Nishiyama, Y.; Miyoshi, T.; Shawkey, M. D.; Dhinojwala, A. Elucidation of the hierarchical structure of natural eumelanins. *J. R. Soc. Interface* **2018**, *15*, 20180045.

(36) Xiong, F.; Han, Y.; Wang, S.; Li, G.; Qin, T.; Chen, Y.; Chu, F. Preparation and Formation Mechanism of Renewable Lignin Hollow Nanospheres with a Single Hole by Self-Assembly. *ACS Sustainable Chem. Eng.* **2017**, *5*, 2273−2281.

(37) Xing, Q.; Buono, P.; Ruch, D.; Dubois, P.; Wu, L.; Wang, W.-J. Biodegradable UV-Blocking Films through Core−Shell Lignin−Melanin Nanoparticles in Poly(butylene adipate-co-terephthalate). *ACS Sustainable Chem. Eng.* **2019**, *7*, 4147−4157.

(38) Bizzarri, B. M.; Martini, A.; Serafini, F.; Aversa, D.; Piccinino, D.; Botta, L.; Berretta, N.; Guatteo, E.; Saladino, R. Tyrosinase mediated oxidative functionalization in the synthesis of DOPA-




https://doi.org/10.1021/acsomega.1c06817
*ACS Omega* 2022, 7, 11722−11730

derived peptidomimetics with anti-Parkinson activity. *RSC Adv.* **2017**, *7*, 20502−20509.
(39) Song, J. E.; Su, J.; Noro, J.; Cavaco-Paulo, A.; Silva, C.; Kim, H. R. Bio-coloration of bacterial cellulose assisted by immobilized laccase. *Amb. Express* **2018**, *8*, 19.
(40) Slagman, S.; Zuilhof, H.; Franssen, M. C. R. Laccase-Mediated Grafting on Biopolymers and Synthetic Polymers: A Critical Review. *ChemBioChem* **2018**, *19*, 288−311.
(41) Aydemir, C.; Yenidoğan, S. Light fastness of printing inks: A review. *Eng. Des.* **2018**, *9*, 37−43.



https://doi.org/10.1021/acsomega.1c06817
*ACS Omega* 2022, 7, 11722−11730